JOURNAL OF CATALYSIS 116, 303–307

A Comparison of Oxidation Activities and Structures of Mo Oxides Highly Dispersed on Group IV Oxide Supports

A number of workers have studied support effects on Mo oxide catalysts. Recently, FTIR and laser Raman studies have revealed the presence of molybdate species highly dispersed on oxide supports (*1–9*). These polymolybdates or molybdate on supports play an important role in desulfurization, metathesis, and oxidation reactions. We have recently reported the characterization and the catalytic activities of such polymolybdates on TiO_2 (*5*), SiO (*6*), and ZrO_2 (*9*). In this note the natures of Mo oxides dispersed on Group IV oxide supports have been compared and the correlation between surface molybdate and the oxidation activity has been discussed.

The Mo oxide catalysts supported on SiO_2, TiO_2, ZrO_2, and GeO_2 were prepared by an impregnation method as reported previously (*5, 6, 9*). Those catalysts were dried at 723 K for 10–22 h. Mo contents ranged from 0.5 to 10 at.% (Mo(0.5)*M* to Mo(10)*M*, *M* = SiO_2, GeO_2, TiO_2, or ZrO_2). GeO_2 was obtained by hydrolysis of $GeCl_4$ in cold water at around 273 K and dried precipitates were heated at 723 K for 4 h. Details of the preparation methods of catalysts were described previously (*5, 6, 9*).

The X-ray diffraction patterns were obtained by a Rigaku Denki RAD-rA diffractometer using Cu$K\alpha$ radiation. A step-scanning method was applied to the quantitative analysis. The IR and Raman spectra of catalysts were recorded on a Shimadzu FTIR 4000 or a JASCO NR-1000 laser Raman spectrometer. Photoluminescence and excitation spectra were measured by a Shimadzu RF-501 spectrofluorophotometer with color filters to eliminate scattered light at 77 K. These experimental procedures were also reported previously (*5, 6, 9*). The oxidative dehydrogenation of ethanol was carried out using a closed circulation system at 453 K. One to five square meters of catalyst was used. The products at 453 K were mainly ethanal and a trace of CO_2 and ethyl acetate. In order to obtain initial rates, conversions were kept below ca. 5% for each catalyst.

The rates of oxidative dehydrogenation of ethanol on Mo–Ge and Mo–Sn together with previous results for Mo–Si (*6*), Mo–Ti (*5*), and Mo–Zr (*9*) are shown in Table 1. The selectivities to CH_3CHO were ca. 90–95% over all the catalysts. Mo–Si and Mo–Ge oxides showed low activities. On the other hand, Mo–Zr, Mo–Ti, and Mo–Sn oxides showed high activities and they increased with increasing Mo loadings up to 5–10 at.% of Mo. The rates on Mo–Ti and Mo–Zr oxide are roughly 20–40 times larger than those on Mo–Si and Mo–Ge oxide.

The amounts of crystalline MoO_3 and noncrystalline Mo oxide on Mo–Ge and on Mo–Sn oxides were estimated by a comparison of the XRD intensities of the catalysts and those in the corresponding physical mixtures of MoO_3 and support oxides by using the method previously applied (*5, 6, 9*). Diffraction lines such as (020), (110), (040), and (021) were integrated at 0.05 intervals of the diffraction angles for 20 s, increasing the signal-to-noise ratio. The fractions of crystalline MoO_3 were calculated by using several diffraction lines and are shown in Table 1.

The concentrations of noncrystalline Mo oxide per surface area are also listed in Table 1. The crystalline MoO_3 showed

0021-9517/89 $3.00

TABLE 1

Estimation of Noncrystalline Mo Oxides and Catalytic Activities

Catalyst (at.%)	Surface area ($m^2\ g^{-1}$)	Fraction of crystalline MoO_3 (%)	Surface concn. of noncrystalline Mo oxide ($\mu mol\ m^{-2}$)	Rate of conv. ($\mu mol\ m^{-2}\ min^{-1}$)[a]	Rate of Mo oxide (min^{-1})[b]
SiO_2[c]	41	—	—	0.00	
Mo(0.5)–Si[c]	41	0	2.0	0.05	0.02
Mo(1)–Si[c]	41	24	3.1	0.23	0.08
Mo(3)–Si[c]	40	90	1.0	0.05	0.05
GeO_2	10–15	—	—	0.004	
Mo(1)–Ge	11	52	3.6	0.18	0.05
Mo(1.9)–Ge	9.5	90	2	0.10	0.05
TiO_2[d]	45	—	—	0.22	
Mo(1)–Ti[d]	45	0	2.6	1.1	0.42
Mo(2.8)–Ti[d]	43	0	8.1	4.6	0.6
Mo(5.8)–Ti[d]	41	12	15	6.9	0.46
ZrO_2[e]	50–70	—	—	0.005	
Mo(1)–Zr[e]	47	0	1.7	0.17	0.1
Mo(3)–Zr[e]	52	0	4.7	4.7	0.5
Mo(5)–Zr[e]	70	0	5.8	5.8	1.2
Mo(10)–Zr[e]	70	22	8.9	8.9	1.0
SnO_2	48			0.53	
Mo(10)–Sn	33	0	36	3.3	0.1 (0.3)
MoO_3	2	100	13	0.8	0.06

Note. p(EtOH) = 6 Torr, $p(O_2)$ = 30 Torr (1 Torr = 133 Pa); Temp 453 K.

[a] Rate per surface area.

[b] Rates are divided by the amount of surface noncrystalline Mo oxide.

[c] Reference (*6*).

[d] Reference (*5*).

[e] Reference (*9*).

sharp XRD lines with narrow half-widths, indicating generally that particle sizes of MoO_3 are above ca. 100 nm (*10*). Although there are some errors in the calculation of the surface concentration of noncrystalline Mo oxide, the amount of noncrystalline Mo oxide on SiO_2 seems to pass through a slight maximum, while the same species on TiO_2 and on ZrO_2 increased with increasing Mo loadings. Assuming 13 $\mu mol/m^2$ as a monolayer of MoO_3, SiO_2 and GeO_2 are covered with MoO_3 at a maximum of 15–30%, while TiO_2 and ZrO_2 are covered at 70–100%. The results suggest that in the case of SiO_2 and GeO_2, Mo oxide favors crystallization to MoO_3 at low Mo loadings, while on TiO_2 and ZrO_2 Mo oxide does not crystallize to MoO_3 until the formation of ca. one monolayer. Similar findings have been reported by Frausen *et al.* (*11*). With SnO_2 support, a large amount of noncrystalline Mo oxide is found. As reported previously (*12*), the presence of Sn ions suppressed the crystallization of Mo oxide. Similar results were also obtained for the Sb–Sn oxide system (*13*).

Both IR and Raman bands of various catalysts together with previous results are listed in Table 2. Mo(1)–Ge showed the bands due to the crystalline MoO_3. We could not observe the IR and Raman bands of polymolybdate species because of severe

TABLE 2

IR and Raman Bands (cm^{-1}) of the Catalysts Calcined at 723 K

Catalyst	IR	Raman
Mo(0.5)–Si	993,[a] 970–940 925–900	997,[a] 980 (broad)
Mo(1)–Si	993,[a] 970–940 880,[a] 925–900	997,[a] 980 (broad) 820[a]
Mo(3)–Si	993,[a] 880[a]	997,[a] 820[a]
Mo(1)–Ge	965(Ge), 880(Ge)	995,[a] 975(Ge), 880(Ge) 820[a]
Mo(1)–Ti	—	950
Mo(2.8)–Ti	950, 905	975
Mo(5.8)–Ti	995,[a] 950, 905	997,[a] 980, 820[a]
Mo(1)–Zr	935	925, 870
Mo(3)–Zr	950	935, 875
Mo(5)–Zr	950, 870	950, 890
Mo(10)–Zr	995,[a] 965, 905	997,[a] 960
Mo(10)–Sn	960	997,[a] 970, 820[a]

[a] The bands due to crystalline MoO_3. (Ge), GeO_2.

overlapping of GeO_2 and Mo oxide bands. With Mo(10)–Sn catalyst, the IR bands are found at 960 cm^{-1} and the Raman bands at 970 cm^{-1} as well as those of MoO_3. The band at ca. 895 cm^{-1} due to tetrahedral Mo species (*14*) could not be observed. As shown in Table 2, some catalysts exhibit Raman bands due to the crystalline Mo oxide. It has been reported that the crystalline phase is considerably more Raman active than the surface phases (*15*). Therefore, the amount of crystalline MoO_3 in Mo(1)–Si, Mo(2.8)–Ti, and Mo(10)–Sn catalysts may be very small.

IR and Raman studies have not discriminated whether surface Mo species are tetrahedral Mo species or octahedral polymolybdate. It has been reported (*6, 16, 17*) that tetrahedrally coordinated Mo species $\left(\begin{matrix}O\\O\end{matrix}\!\!=\!\!Mo\!\!<\!\!\begin{matrix}O-\\O-\end{matrix}\right)$ on supports exhibit a maximum in the excitation at 260–280 nm and in the emission at 460–490 nm which has been attributed to the charge-transfer process $[(Mo^{6+}{=}O^{2-}) \rightleftharpoons^{h\nu}_{h\nu'} (Mo^{5+}{=}O^{-})^*]$. Tetrahedral Mo ions in the Mo–Si oxides containing 0.5–3 at.% Mo have been estimated from the emission spectra at 480 nm and the excitation at 290 nm. It has been implied that the intensity of the photoluminescence of the Mo–Si oxide is proportional to the concentration of tetrahedral Mo ions as reported previously (*6, 17*). The fractions of tetrahedral Mo ions in Mo(0.5)–Si, Mo(1)–Si, and Mo(3)–Si oxide have been estimated as ca. 25–70, 6–15, and 2–3%, respectively, from a comparison of the photoluminescence intensities between these catalysts and Mo oxide grafted onto SiO_2 which seems to contain only isolated tetrahedral Mo species (*6*).

Similar methods were applied to the Mo–Zr, Mo–Ti, and Mo–Ge systems. As shown in Fig. 1, with Mo(1)–Zr and Mo(1)–Ge, weak emission maxima at around 490 nm and excitation maxima at around 290 nm were observed. These bands seem to originate from the presence of isolated tetrahedral Mo species as in the Mo–Si system (*6*). These intensities are very weak compared to those of Mo–Si oxide. If a comparison may be allowed under the assumption of equal probability in radiationless deactivation from charge-transfer excited states between these systems, the concentration of tetrahedral Mo species on Mo(1)–Ge and Mo(1)–Zr is below 1%. In the case of Mo–Ti catalysts, the spectra of Mo species

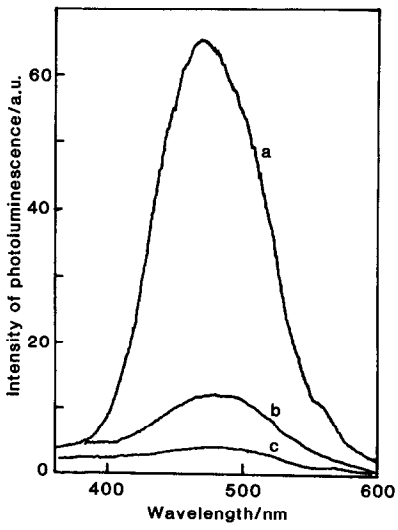

FIG. 1. Photoluminescence spectra of catalysts. (a) Mo(1)–Si, (b) Mo(1)–Ge, (c) Mo(1)–Zr. Photoluminescence spectra were measured by 280-nm excitation at 77 K.

TABLE 3

Some Properties of Group IV Oxides and Their Cations

Support	Crystal type	Coordination number of cation	Ionic radius[a] (pm)	Surface polymolybdate formation	Isolated tetrahedral molybdate
SiO_2	Amorphous	4	38	+[c]	+
GeO_2	Low quartz	4	54		
TiO_2	Anatase	6	60	+++	
ZrO_2	Monoclinic	7[b]	77	+++	
SnO_2	Rutile	6	71	+++	
Isolated molybdate		4	60		
Polymolybdate		6	60		

[a] By Goldschmidt.
[b] See Ref. (*18*).
[c] Denotes the extent of formation.

could not be obtained because of the UV absorption overlap due to TiO_2 itself.

As just described above, Mo–Ti and Mo–Zr oxides contain a large amount of noncrystalline Mo oxides. Considering that tetrahedral Mo species on Mo(1)–Zr is below 1% of Mo species, with Mo(3)–Zr to Mo(10)–Zr oxide major species seem to be polymolybdate. The same situation seems to be applicable for Mo–Ti oxides. With Mo–Si oxide, a large amount of isolated tetrahedral Mo species and a small amount of polymolybdate and crystalline MoO_3 are confirmed on SiO_2. Considering that only 15–30% of the surface is covered with noncrystalline Mo oxide, it is suggested that the interaction of Mo oxide with SiO_2 is significantly different from that with TiO_2 or ZrO_2.

Table 3 shows some properties of support oxides and their cations together with Mo species. The structures of both crystalline modifications of silica and amorphous silica can be visualized as a network of interlinked SiO_4 tetrahedra. Their cation sizes are 40–50 pm. The structures of both TiO_2 and ZrO_2, which are very effective supports for polymolybdate formation, are octahedrally or heptahedrally (*18*) coordinated. Their cation sizes are 60–80 pm. Mo^{6+} ions of polymolybdate are probably coordinated octahedrally and its size is ca. 60 pm. The coordination and sizes of Mo^{6+} resemble those of TiO_2 and ZrO_2 rather than that of SiO_2. As described above, TiO_2 and ZrO_2 are favorable for formation of octahedral polymolybdate up to 5–10 at.% of Mo, i.e., ca. one monolayer. SiO_2 is favorable for formation of isolated tetrahedral Mo species at low Mo content and makes the crystalline MoO_3 rather than octahedral polymolybdate at higher Mo content. According to these situations, SnO_2 support resembles TiO_2 and ZrO_2 and GeO_2 support resemble SiO_2.

Since samples of parent GeO_2, TiO_2, and ZrO_2 showed low activity for ethanol oxidation, as shown in Table 1, it is apparent that molybdenum ions act as active sites for oxidation reaction. In this work, three types of Mo oxides, i.e., isolated tetrahedral species, polymolybdate, and crystalline MoO_3, have been found in the catalysts. Although we cannot give a complete explanation about the nature of such species, some features can be seen. The contribution of crystalline MoO_3 to the oxidation activity seems to be negligible, since the surface area of crystalline MoO_3 to the total surface area is very small in each case. The Mo–Si oxides contain both isolated tetrahedral Mo species and polymolybdate. Tetrahedral spe-

cies may have low activity for oxidative dehydrogenation, since Mo(0.5)–Si showed very low activity for it. Iwasawa *et al.* have reported that the isolated tetrahedral Mo ions are less active for oxidative dehydrogenation than species where two adjacent Mo are present (*19*). As shown in Table 1, the activity of surface Mo species on Mo–Si and on Mo–Ge is much smaller than those on TiO_2 and ZrO_2. High activities on Mo–Ti or Mo–Zr oxides seem to originate from polymolybdate. With Mo(10)–Sn oxide catalyst, the amount of noncrystalline Mo is very high and corresponds to ca. three layers. The rate per surface Mo species over this catalyst may be estimated to be ca. 0.3 rather than 0.1 min^{-1}.

ACKNOWLEDGMENTS

The authors thank Dr. M. Anpo for measurements of photoluminescence spectra and Dr. T. Ohno (Kobe University) for FTIR measurements.

REFERENCES

1. Medema, J., Van Stam, C., De Beer, V. H. J., Konings, A. J., and Koningsberger, D. C., *J. Catal.* **53,** 386 (1978).
2. Zingg, D. S., Makovsky, R. E., Tisher, R. E., Brown, F. R., and Hercules, D. M., *J. Phys. Chem.* **84,** 2898 (1980).
3. Seyedmonir, R. S., Abdo, S., and Howe, R. F., *J. Phys. Chem.* **86,** 1233 (1982).
4. Rodrigo, L., Marcinkowska, K., Adnot, A., Roberge, P. C., Kaliaguine, S., Stencel, J. M., Makovsky, L. E., and Diehl, J. R., *J. Catal.* **95,** 414 (1986).
5. Ono, T., Nakagawa, Y., Miyata, H., and Kubokawa, Y., *Bull. Chem. Soc. Japan* **57,** 1205 (1984).
6. Ono, T., Anpo, M., and Kubokawa, Y., *J. Phys. Chem.* **90,** 4780 (1986).
7. Quincy, R. B., Honalla, M., and Hercules, D. M., *J. Catal.* **106,** 85 (1987).
8. Ramis, G., Busca, G., and Lorenzelli, V., *Z. Phys. Chem. Neue Folge* **153,** 189 (1987).
9. Ono, T., Miyata, H., and Kubokawa, Y., *J. Chem. Soc. Faraday Trans. 1* **83,** 1761 (1987).
10. For example, Nitta, I., *in* "X-sen Kesshougaku," p. 480. Maruzen, Tokyo, 1975.
11. Frausen, T., Van Berge, P. C., and Mars, P., "Preparation of Catalysts 1" (G. Poncelet and P. A. Jacobs, Eds.). Elsevier, Amsterdam, 1976.
12. Ono, T., Ikehata, T., and Kubokawa, Y., *Bull. Chem. Soc. Japan* **56,** 1284 (1983).
13. Ono, T., Yamanaka, T., Kubokawa, Y., and Komiyama, M., *J. Catal.* **109,** 423 (1988).
14. Busey, R. H., and Keller, O. L., *J. Chem. Phys.* **41,** 215 (1964).
15. For example, Chan, S. S., Wachs, I. E., and Murrell, L. L., *J. Catal.* **90,** 150 (1984).
16. Iwasawa, Y., and Ogasawara, S., *Bull. Chem. Soc. Japan.* **53,** 3709 (1980); Kazanskii, V. B., *Kinet. Catal.* **24,** 1338 (1983).
17. Anpo, M., Tanahashi, I., and Kubokawa, Y., *J. Chem. Soc. Faraday Trans. 1,* **78,** 2121 (1982); Anpo, M., Tanahashi, I., and Kubokawa, Y., *J. Phys. Chem.* **86,** 1 (1982); Kubokawa, Y., and Anpo, M., "Adsorption and Catalysis on Oxide Surfaces" (M. Che and G. C. Bond, Eds.), p. 127. Elsevier, Amsterdam, 1985.
18. Wells, A. F., "Structural Inorganic Chemistry," p. 449. Clarendon Press, Oxford, 1975.
19. Iwasawa, Y., and Tanaka, H., *in* "Proceedings, 8th International Congress on Catalysis, Berlin, 1984," Vol. IV, p. 381. Dechema, Frankfurt-am-Main, 1984; Iwasawa, Y., "Advances in Catalysis," Vol. 35, p. 250. Academic Press, New York, 1987.

T. ONO[1]
H. KAMISUKI
H. HISASHI
H. MIYATA

Department of Applied Chemistry
University of Osaka Prefecture
Sakai, Osaka 591, Japan

Received January 4, 1988; revised September 13, 1988

[1] To whom correspondence should be addressed.